Properties of NBR and CR Hyperelastic Materials in a Wide Range of Both Positive and Negative Temperatures

Marcin Konarzewski[1], Michał Stankiewicz[1], Robert Panowicz[1], Marcin Sarzyński[2], Marcin Wieczorek[1]

[1]Faculty of Mechanical Engineering, Military University of Technology, Sylwestra Kaliskiego Street 2, 00-908, Warsaw, Poland; marcin.konarzewski@wat.edu.pl (M.K.), michal.stankiewicz@wat.edu.pl (M.S.), robert.panowicz@wat.edu.pl (R.P.), marcin.wieczorek@wat.edu.pl (M.W.)

[2]Faculty of Mechatronics and Aeronautics, Military University of Technology, Sylwestra Kaliskiego Street 2, 00-908, Warsaw, Poland; marcin.sarzynski@wat.edu.pl (M.Sz.)

Abstract: Hyperelastic materials are widely used in many industries. Their use requires thorough knowledge of their strength parameters over a wide temperature range. However, determination of the parameters of hyperelastic materials is still a challenge. Therefore, the paper presents research methodology allowing determination of the properties of hyperelastic materials in a wide range of stretch and temperatures (from +50°C to -25°C) on the example of NBR (nitrile butadiene rubber) and CR (chloroprene rubber) elastomers. On the basis of physical premises, a hyperelastic constitutive model was also modified through introducing an explicit dependence of strain energy on temperature, allowing an accurate reflection of the properties of the tested materials. The material parameters of the adopted strain energy functions for the NBR and CR were determined with R2 not less than 0.999.

Keywords: elastomers; polymers; uniaxial tension; temperature effects; failure

1 Introduction

Nowadays, hyperelastic materials are as often used in industry as other, more traditional materials. Particularly the automotive industry shows its great interest in this type of materials. In addition to their main application, i.e., for car tires, elastomers are used as vehicle suspension components, engine vibration dampers, and sealing in various types of connections. Hyperelastic materials are also used in other industries, including civil engineering, aviation or also biomechanics.

Due to such a wide spectrum of a usage of hyperelastic materials, it is crucial to precisely determine their mechanical properties. Hyperelastic materials, similarly as other elastomers in general, are polymers in which polymer chains are joined by intermolecular bonds. It should be noted that due to their internal structure, those materials properties, such as tensile strength, stiffness or stress, change depending on the temperature [1-3]. This relationship was not noticed at the beginning, therefore, their parameters were initially determined only in an ambient temperature. In a later period of the experimental studies this influence taken into account, however, mainly in the range of positive temperatures [4-9]. It could be assumed that as the temperature increases, much larger displacements and elongation of the sample are obtained. However, in the case of hyperelastic materials, at elevated temperatures, there occurs a rapid degradation of polymer chains as well as their weakening and breaking. For this reason, higher elongation values are obtained for negative temperatures [10]. This phenomenon only occurs to a certain limit called the brittleness temperature [11]. Thus, testing properties of this type of materials over a wide temperature range is crucial.

There is a whole range of hyperelastic materials differing significantly in their mechanical properties and, thus, their usage [12]. The presented article focuses on two commonly used materials, namely, NBR (nitrile butadiene rubber) and CR (chloroprene rubber) rubbers. NBR, which is a copolymer of acrylonitrile and butadiene, is characterised by an excellent resistance to a wide range of oils of mineral, animal and vegetable origin as well as to fuels and other chemicals [13]. It is an elastic material with a high tensile strength and a low compression deformation [14]. For this reason, it is frequently used in the automotive or aviation industry, to produce seals (for both hydraulic and pneumatic installations), vibration damping elements and self-sealing fuel tanks. This material owes its oil-resistant properties to the presence of nitrile: the greater the proportion of nitrile, the better the resistance to chemicals while reducing the flexibility [15]. A theoretical range of the operating temperature is between -40°C and 110°C [16].

CR is a synthetic material created in the process of polymerisation of chloroprene [17]. This material is characterised by high resistance to weather conditions, ozone and even to weak acids. Due to high chemical stability, it is relatively well resistant to aging [18]. It shows some resistance to oils and fuels, however, not as strong as NBR rubber does. Due to its properties, it is widely used for production of gaskets for joints exposed to environmental and corrosive factors. However, the most common use is the production of all kinds of wetsuits since CR provides very good insulation form the cold. In the case of CR, the maximum operating temperature is about 80°C.

While analysing available literature on the subject, it can be concluded that a relatively small number of publications concern the testing of material properties of rubber materials at both positive and negative temperatures [19]. For example, in work [20], the authors analyse butadiene rubber filled with carbon black, subjected to dynamic loading at three temperatures: -40, 20 and 70°C. Based on the results

obtained from experimental studies the authors proposed a new constitutive model for finite rubber viscoelasticity. In paper [21] the results of tests on the dependence of temperature on mechanical properties of the reinforced rubber are presented. In this paper, the range from -20 to 100°C was considered and cylindrical samples were tested. Two thermocouples were used to control the sample temperature during the tests: one was attached to the external surface of the sample, the other was placed in a hole drilled in the centre of the sample. It was found that the temperature equilibrium was obtained after about 20 minutes from placing the sample in the temperature chamber. The research showed that both the elastic and the rate dependent properties depend on the temperature: the elastic behaviour is determined by entropy elasticity, whereas the viscous behaviour by a non-linear temperature dependent viscosity. In [22], the authors analysed silicone elastomer filled with silica. Uniaxial tension and shear tests were performed in a wide range of temperatures (from -55 to 70°C). Similarly to other works, the dependence of the temperature on the material properties was confirmed.

The basic experimental test, not only in the case of hyperelastic materials, is the tensile test [10, 23-25]. In the case of elastomers, due to significant deformations that they undergo, measuring mechanical parameters is a more difficult issue than in the case of traditional materials. The use of traditional extensometers in this case is significantly limited, therefore, it is necessary to utilise specialized extensometers for high elongations [25] or optical and digital image correlation (DIC) methods [26, 27]. The DIC method assumes the use of a series of markers, placed on the tested sample, whose position change during the test is recorded by an optical device (e.g., video camera). The recorded images are compared with each other and the desired parameters are determined on this basis. The use of each of the abovementioned methods has some advantages as well as limitations. The extensometers need to be placed near the sample since in the case of tests with use of a small-scale temperature chamber their use can be difficult due to low space. In addition, their operating temperature is in the range of -40°C to 80°C, due to the properties of the material from which the measuring element is made (usually in the form of a long tape, attached to the tested sample). The use of DIC methods requires special preparation of the surface of the tested samples by applying the measuring points or a layer of paint, in such a way that they are clearly visible in the camera lens throughout the test. Testing in sub-zero temperatures also requires proper preparation of the observation field to prevent frost build-up.

Hyperelastic materials are used in a wide range of temperatures, both positive and negative. In the literature it is possible to find descriptions and results of studies on the impact of positive temperatures on the properties of such materials, however, in the case of the negative temperatures there are much less publications on this subject. In addition, the number of constitutive models describing the behaviour of hyperelastic materials with regard to the thermal load is relatively small.

The main aim of presented article is to show the impact of a wide range of temperatures on the properties of CR and NBR materials. The selected temperature

range corresponds to the typical operating conditions of such materials. In addition, numerical models are currently used in many research areas, so an attempt was made to modify the constitutive model of hyperelastic materials by a part describing the effect of the thermal load.

2 Materials and Methods

2.1 Speciment Preparation

As it was mentioned earlier, two materials commonly used in the industry were selected for the research: NBR and CR. The test materials were delivered in the form of premade 300x300 mm and 2 mm thick sheets. The composition of tested materials is presented in the Table 1. The dimensions of the samples were determined on the basis of the PN-ISO 37:2007 standard concerning determination of the tensile properties of rubber (Fig. 1). The water jet cutting technique was used to prepare the test samples presented in Fig. 2.

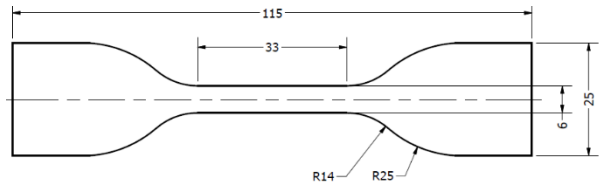

Figure 1
Dimensions of the test samples according to the PN-ISO 37:2007 standard

Table 1
Composition of tested hyper elastic materials (phr - weight parts per 100 parts of rubber)

Component [phr]	**CR**	**NBR**
Chloroprene rubber (Denka S-40)	100	-
Acrylonitrile-butadiene rubber (Ker N-29)	-	100
Carbon black (N-550)	45	50
Crosslinking complex (sulfur, ZnO, et al.)	-	13,6
Crosslinking complex (MgO, ZnO, et al.)	14,6	-
Softener (ADO or AN-68*)	10	15
Hardness Shore A (at 21°C)	65	62

White paint markers were applied on every sample in the measuring part. It was necessary to determine the deformations of the samples during the tensile test using a motion tracking method.

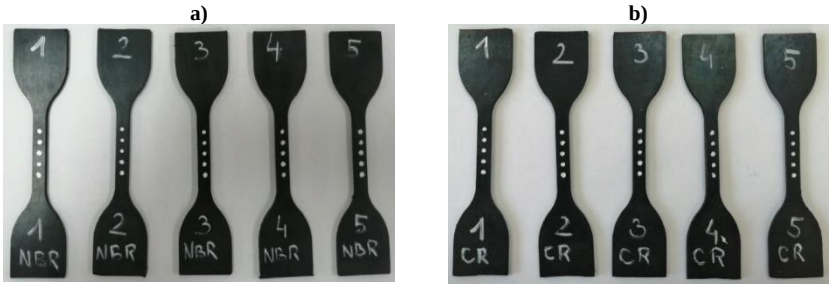

Figure 2
Test samples: (a) NBR; (b) CR

2.2 Tensile Test Method

The test was carried out on the MTS Criterion Model 45 electromechanical universal test system (Fig. 3). The maximum displacement range was ± 500 mm and the maximum piston speed was 750 mm/min. During the test, LED lighting (Fig. 4a) was used to increase the brightness and quality of the recordings.

Tests in negative and positive temperatures were carried out using the ThermCraft temperature chamber, installed on the MTS test system, which allows conducting the test at temperatures from -150°C to 320°. To reduce the temperature in the chamber below the ambient temperature, liquid nitrogen fed from a Dewar cryogenic storage was used (Fig. 3).

The test system automatically recorded the loading force and the position of the traverse in time with 50 Hz frequency. The tests were performed by applying displacement-controlled loading. The speed of the traverse was equal to 50 mm/min and a strain rate during the test was constant and equal to $3.3 \cdot 10^{-2}$ 1/s. The forces recorded by the test system along with the displacements determined using the motion tracking method allowed for determination of strain and stress curves for all considered samples.

The tensile tests were carried out on the basis of the PN-ISO 37:2007 standard. According to the standard the tests are performed with use of the dog bone samples at a constant strain rate. The test samples can be formed directly at the manufacturer or cut out from the premade sheets. Tensile stress is calculated as the force related to the initial cross-section area of the gage length of the tested sample. Tensile strength is defined as the maximum recorder tensile stress and elongation at break as the gage length deformation at break. The effect of transverse deformations of the sample during the test is not taken into account.

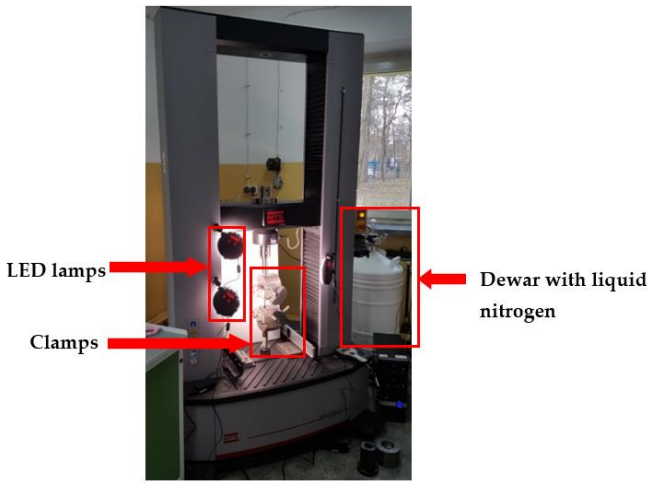

Figure 3
MTS Criterion Model 45 universal test system

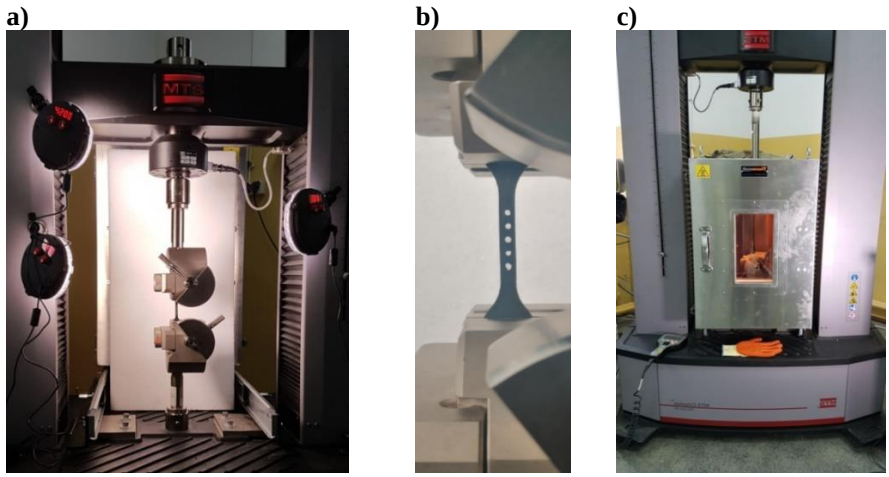

Figure 4
Sample installed in the test system clamps:
(a) general view; (b) close-up of a sample; (c) temperature chamber

The samples were tested in the following temperature range: -25°C, 0°C, 25°C, 50°C. After mounting the samples in the clamps of the testing system and closing the climate chamber, about 10 minutes were allowed to settle and normalize the temperature inside the chamber. Measurements of the temperature inside the chamber were performed by using the two K type thermocouples: one placed in the working field of the chamber and the other fixed between two layers of the tested material (two pieces of the test material were applied to each other and a

thermocouple was placed between them). The tests were carried out when the control system was showing a constant, set temperature. According to the chamber specification it allows temperature stabilization in the range of ±1°C, and the permissible K type thermocouple error is ±1.5°C.

At the ambient temperature 5 samples of every material were tested, while in other temperatures it was 3 samples.

The motion tracking method was used to determine the deformation of the samples during the tensile tests. Each test was recorded using a high resolution (1920x1080 px) camera with a speed of 25 frames/second. The recorded movies were imported into the TEMA software and then subjected to the image analysis. Figure 5a presents a sample with markers used as measuring points (Fig. 5b). During the image analysis process three points were tracked by the software and a change of their coordinates in time was recorded. The example of the motion tracking process for the sample during the tensile test is presented in Fig. 5c. It can be observed that markers are stretching along with the sample; however the measuring points are located in the centre of the markers during the whole test procedure. Based on the obtained data, the strains of the samples were calculated.

a)

b)

c)

Figure 5
Method of strain determination measurement: (a) sample with visible markers; (b) measurement points; (c) sample during the analysis process

3 Results

As it was mentioned earlier the tensile test was performed on the NBR and CR materials. In Figure 6, the samples destroyed during the tests at the ambient temperature are presented.

Figure 6
Test samples: (a) NBR; (b) CR

The stresses, determined with the use of the motion tracking method, for all 5 samples of both tested materials at the ambient temperature are presented in Fig. 7. It can be observed that all the curves are located in relatively narrow range. The standard deviation of extension for CR is only 0.1 and 0.17 for NBR. On this basis, it was found that at the remaining temperatures only 3 samples made from each material will be tested.

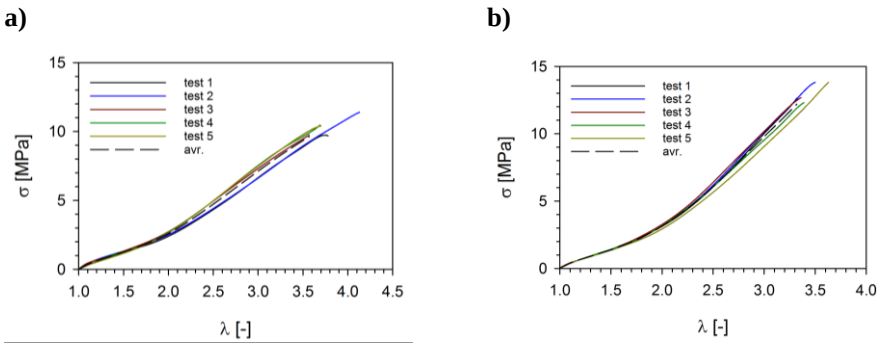

Figure 7
Stress-extension curves for tests at the ambient temperature: (a) NBR ; (b) CR

The averaged curves of stress-extension rate for tests performed in the considered range of temperatures are presented in Fig. 8.

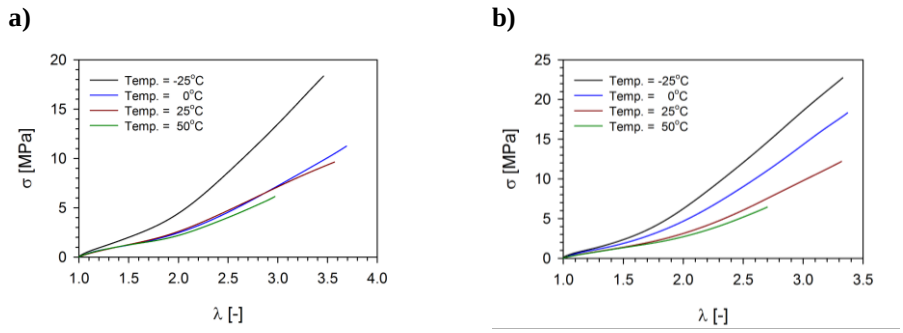

Figure 8

Stress-extension curves for a wide range of temperatures: (a) NBR; (b) CR

Analysing the above graphs, it can be observed that the curves for the NBR material for temperatures in the range from 0 to 50°C are very similar. Up to extension $\lambda=2$ the curves practically coincide. When $\lambda>2$ a change in the slope of the curve representing tests at 50°C can be observed, whereas the curves for 0 and 25°C continue to coincide until they are finally separated at $\lambda=3$. Such behaviour means that NBR is characterised by similar stiffness in this temperature range. The difference in the maximum stresses, and thus in the strength, results from the degradation process of the polymer chains in the material. This process occurs faster as the thermal load of the sample increases, therefore, the lowest strain value (6 MPa) was obtained at 50°C.

At -25°C there is a significant change in the stiffness and strength of the NBR material. The maximum stress was 19 MPa, which is almost a twofold increase compared to the stress at 0°C (10 MPa). The maximum extension λ was about 3.4, similarly to the values obtained from temperature of 0□C. It resulted from to the fact that in these cases the sample was not fractured due to a limited movement range of the test system traverse caused by the size limitation of the used temperature chamber.

In the case of the CR material it can be observed that only the curves for ambient and 50°C temperatures coincide to the value of the extension of about 1.8. In other cases the distribution of the stress-extension curves is even and a difference in the maximum stress is about 6 MPa. For the ambient temperature, the maximum obtained stress was 12 MPa, for 0°C it was about 18 MPa, while the maximum value of 23 MPa was obtained for a temperature of -25°C. Therefore, there is no rapid change in the stiffness after exceeding a certain critical temperature.

The influence of the temperature on both NBR and CR samples stretching process is also presented in Fig. 9. It shows a relationship between the stress and the temperature for selected extension values. In the case of the NBR (Fig. 9a), a change

in the temperature influence occurs at 0°C, whereas in the case of the CR (Fig. 9b) at 25°C. Above these values the temperature has a significantly smaller effect on the stress of the deformed material.

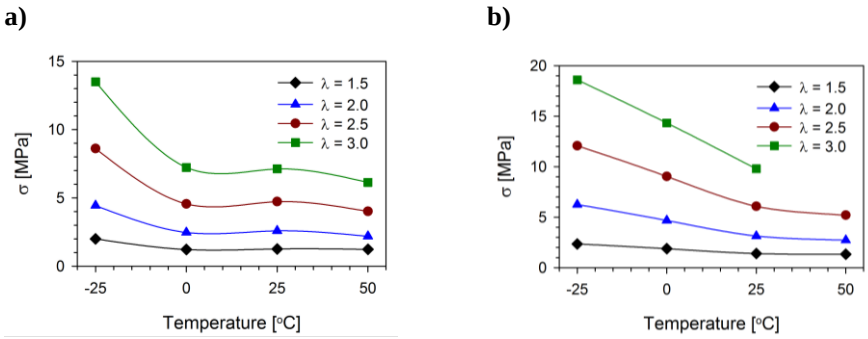

Figure 9
Stress-temperature curve for different values of extension (a) NBR; (b) CR

Such effects is also seen in Fig. 10. Stress-extension curves for 0°C and 25°C temperatures in the case of the NBR practically coincide. However, in the case of the CR material a significant influence of the temperature can be observed. It should be noted that despite, such a different impact of the temperature in both cases, the maximum deformation increases with a decrease in temperature.

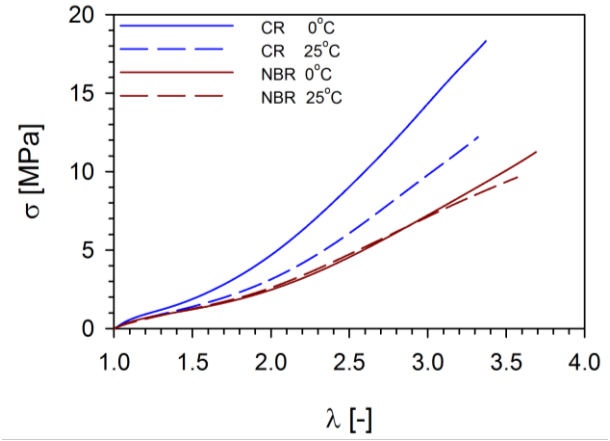

Figure 10
Stress-extension curves for selected temperatures

3 Hyperelastic Constitutive Models

The behaviour of hyperelastic material is usually described by means of the Cauchy stress tensor [28]:

$$\tilde{\sigma} = 2\frac{\tilde{B}}{\sqrt{I_3}}\frac{\partial W}{\partial \tilde{B}} = 2\frac{\tilde{B}}{\sqrt{I_3}}\left(\frac{\partial W}{\partial I_1}\frac{\partial I_1}{\partial \tilde{B}} + \frac{\partial W}{\partial I_2}\frac{\partial I_2}{\partial \tilde{B}} + \frac{\partial W}{\partial I_3}\frac{\partial I_3}{\partial \tilde{B}}\right)\tilde{\sigma} = 2\frac{\tilde{B}}{\sqrt{I_3}}\frac{\partial W}{\partial \tilde{B}} = 2\frac{\tilde{B}}{\sqrt{I_3}}\left(\frac{\partial W}{\partial I_1}\frac{\partial I_1}{\partial \tilde{B}} + \frac{\partial W}{\partial I_2}\frac{\partial I_2}{\partial \tilde{B}} + \frac{\partial W}{\partial I_3}\frac{\partial I_3}{\partial \tilde{B}}\right) \quad (1)$$

$$I_1 = tr\tilde{B} \quad (2)$$

$$I_2 = \frac{1}{2}\left[I_1^2 - tr\left(\tilde{B}^2\right)\right] \quad (3)$$

$$I_3 = det\tilde{B} \quad (4)$$

where: $\tilde{B}$ is the left Cauchy – Green tensor, I_i (i = 1, 2, 3) are strain invariants, W is strain energy function dependent on strain invariants $W(I_1, I_2, I_3)$.

Derivatives of strain energy functions occurring on the right side of equation (1) can be described by the following relationships:

$$\frac{\partial I_1}{\partial \tilde{B}} = \tilde{I} \quad (5)$$

$$\frac{\partial I_2}{\partial \tilde{B}} = I_1\tilde{I} - \tilde{B} \quad (6)$$

$$\frac{\partial I_3}{\partial \tilde{B}} = I_2\tilde{I} - I_1\tilde{B} + \tilde{B}^2 \quad (7)$$

For incompressible material, what is conventional assumption for hyperelastic materials, taking into account (5) - (7) the Cauchy stress tensor (1) takes the form:

$$\tilde{\sigma} = -p\tilde{I} + 2\left(\frac{\partial W}{\partial I_1} + I_1\frac{\partial W}{\partial I_2}\right)\tilde{B} - 2\frac{\partial W}{\partial I_2}\tilde{B}^2 \quad (8)$$

where p is pressure.

The assumption of rubber incompressibility also limits the number of variables on which strain energy functions depends (I_3 = 1, to $W(I_1, I_2)$).

Strain energy functions should allow reflecting the behaviour of hyperelastic material including dependence on symmetry, thermodynamic, energetic and entropic considerations in the whole range of extension variability. Functions should also meet certain conditions [29]:

1. Energy vanishes in the undeformed configuration:

$$W|_{I_1=3} = 0 \quad (9)$$

2. strain energy functions and stress tends to infinity at very large deformation:

$$\lim_{\lambda_i \to 0} W = +\infty, \lim_{\lambda_i \to 0} \frac{\partial W}{\partial \lambda_i} = -\infty, \tag{10}$$

$$\lim_{\lambda_i \to +\infty} W = +\infty, \lim_{\lambda_i \to +\infty} \frac{\partial W}{\partial \lambda_i} = +\infty, \tag{11}$$

3. stress is equal to zero in the undeformed configuration and strain energy functions achieves minimum

$$\left.\frac{\partial W}{\partial \lambda_i}\right|_{\lambda_1=\lambda_2=\lambda_3=1} = 0, \left.\frac{\partial^2 W}{\partial \lambda_i^2}\right|_{\lambda_1=\lambda_2=\lambda_3=1} > 0, \; det\left[H_{ij}\right] > 0, \tag{12}$$

where: H_{ij} is Hessian matrix and i, j =1, 2, 3

Numerous articles are devoted to the problems associated with the definition of strain energy functions. Those articles present phenomenological approach [30-33], theoretical approach using statistical mechanics of molecular chains network [34, 35] or a mixed approach.

Based on the kinetic theory of elasticity developed by Wall [36], Treloar defined the simplest form of strain energy functions commonly known as neo-Hookean model [37]:

$$W = \frac{\mu}{2}(I_1 - 3) \tag{13}$$

where: m is shear modulus.

The value of the shear modulus is related to the temperature and chain density dependence:

$$\mu = nkT \tag{14}$$

where: *k* is Boltzmann constant, *T* is temperature, *n* is chain density.

This relationship shows that strain energy functions *W* are dependent on temperature. In [37] Xu Li and others used a model for thermal deformation to show that m can be described with a good approximation as the square function of temperature:

$$\mu = \mu_0 \left[1 + C_{T1}\frac{\Delta T}{T_0} + C_{T2}\left(\frac{\Delta T}{T_0}\right)^2\right] \tag{15}$$

where: T_0 is a reference temperature, DT = T - T_0, , T is a temperature at which the experiments were carried out, m_0 is shear modulus at T_0 temperature, C_{T1}, C_{T2} are materials constants.

Arruda and Boyce [34, 35], using phenomenological approach, developed a model with other material constants dependent on temperature assuming their linear temperature dependence. They also showed that the adopted model successfully reflects the behaviour of tire rubbers even at relatively high temperatures and under a moderate finite deformation.

Using the above-described approach, an explicit dependence of the strain energy function on temperature was introduced to the equation [38]:

$$W = A\{exp[m_A(I_1 - 3)] - 1\} + B\{exp[m_B(I_2 - 3)] - 1\} \tag{16}$$

which after modification took the form of:

$$W = \left[A_0 + A_{T1}\frac{\Delta T}{T_0} + A_{T2}\left(\frac{\Delta T}{T_0}\right)^2\right]\{exp[m_A(I_1 - 3)] - 1\} + \left[B_0 + B_{T1}\frac{\Delta T}{T_0} + B_{T2}\left(\frac{\Delta T}{T_0}\right)^2\right]\{exp[m_B(I_2 - 3)] - 1\} \tag{17}$$

The modified equation (17) as well as equation (16) meet conditions 1-3 described before.

Equation (17) was chosen with a trial-and-error method using the review work [37] thus R^2 and RMSE in the case of tested materials reach the largest and smallest value, respectively in the whole range of temperatures considered with the smallest number of material parameters.

Based on the experimental tests the determination of the material parameters is carried out by minimizing the functional:

$$g = min\left[\sum_i^k \left(y_{\exp i} - y_{num\,i}\right)^2\right] \tag{18}$$

where: $y_{exp\,i}$ – i-th measured experimental quantity, $y_{num\,i}$ – i-th calculated function value, k – number of measuring points.

Process of minimizing the functional is accomplished using a non-linear least squares method [39] and in particular using the Levenberg–Marquardt (LM) method [40-42].

In accordance with the methodology presented in [33], initially the parameters A_0, B_0, m_{A0} and m_{B0} were determined by analysing the reference temperature T_0 = 25 C. Then, using the experimental results for temperatures different from the reference temperature, other material constants were determined (A_{T1}, A_{T2}, B_{T1}, B_{T2}) using the LM algorithm and Matlab software. In the case of both tested materials the last term of equation (17) dependent on the invariant I_2 is almost a linear function of the temperature. Therefore, B_{T2} = 0 was adopted. The obtained material parameters are presented in Table 2. In each considered case R^2 was greater than 0.999, while the RMSE was less than 0.1.

Table 2

Determined material parameters

	A_0	A_{T1}	A_{T2}	m_A	B_0	B_{T1}	m_B	R^2	RMSE
NBR	0.353	-0.963	4.221	0.03112	0.2804	1.675	-3.928	0.9997	0.03
CR	0.3917	-1.228	6.782	0.06884	0.2886	0.9735	-4.134	0.999	0.1

The comparison of the experimental results with the results of the calculations for the reference temperature is presented in Fig. 11. The obtained parameters allow for a good mapping of the behaviour of the tested materials in the entire range of temperatures and deformations. The accuracy of the approximation decreases at the negative temperatures at which the rubber properties change significantly.

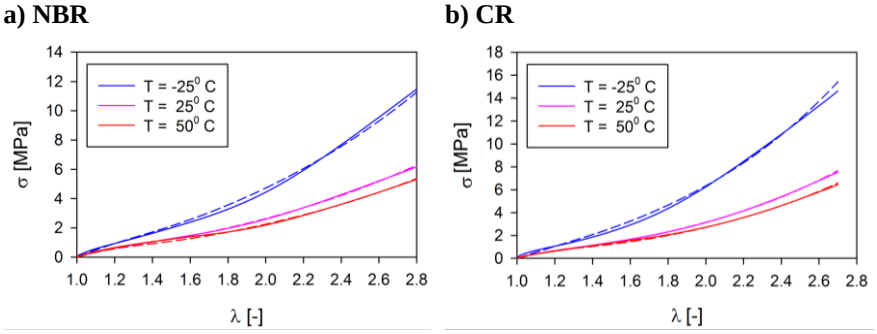

Figure 11

Comparison of the experiment (solid line) and numerical (dashed line) stress-extension curves: (a) NBR; (b) CR

Conclusions

The article presents the results of the research on the NBR and CR hyperelastic materials. Static tensile tests were carried out in the wide range of temperatures (-25, 0, 25, 50°C) using a temperature chamber. The motion tracking technique was used to determine the deformation of the samples. Analysing the obtained results it can be concluded that:

- the strain-extension curves for the NBR are similar in the range of 0-50°C. No change in the NBR stiffness was observed in this temperature range contrary to the temperature of -25°C at which strength and stiffness increased significantly;
- the maximum achieved stress for the NBR material was 19 MPa (for temperature -25°C), while the lowest value of 6 MPa was obtained at 50°C with extension λ=3;
- the stress-extension curves for the CR material for the ambient temperature and 50°C coincide up to the value of the extension of 1.8. For other temperatures the distribution of the curves is even;
- the maximum stress of 23 MPa was obtained for the temperature of -25°C temperature, whereas for the 50°C a value of the stress was about 6 MPa;
- at temperature of 50°C there is a significant reduction in strength for both the tested hyperelastic materials.
- the CR in the considered temperature range is characterised by a greater strength than the NBR, while maintaining the same extension as the NBR.

On the basis of the experimental data the hyperelastic constitutive model was also modified by introducing an explicit dependence of strain energy on the temperature, allowing to accurately reflect the properties of the tested materials. The material parameters of the adopted strain energy functions for the NBR and CR were determined with R^2 not less than 0.999.

The results presented in the article do not exhaust the hyper elastic materials issue. Further research is needed in order to accurately determine the properties and behaviour of such materials in various loading conditions and temperatures. Examples of such tests can be tensile tests at temperatures below -25°C in order to determine the brittleness temperature, compression tests in the range of high strain rates with simultaneous thermal load or biaxial tensile tests.

Acknowledgement

This research was funded under the Project of the Ministry of National Defense of the Republic of Poland Program - Research Grant (GBMON/13-999/2018/WAT) and the article was written as part of the implementation of the university research grant No 22-750 of Military University of Technology.

References

[1] Li, X.; Dong, Y.; Li, Z.; Xia, Y. EXPERIMENTAL STUDY ON THE TEMPERATURE DEPENDENCE OF HYPERELASTIC BEHAVIOR OF TIRE RUBBERS UNDER MODERATE FINITE DEFORMATION. *Rubber Chem. Technol.* **2011**, *84*, 215-228, doi:10.5254/1.3577534

[2] Treloar, L. R. G. *The physics of rubber elasticity*; Oxford classic texts in the physical sciences; 3rd ed.; Clarendon Press ; Oxford University Press: Oxford : New York, 2005; ISBN 978-0-19-857027-1

[3] Smith, T. L. Dependence of the ultimate properties of a GR-S rubber on strain rate and temperature. *J. Polym. Sci.* **1958**, *32*, 99-113, doi:10.1002/pol.1958.1203212409

[4] Bell, C. L. M.; Stinson, D.; Thomas, A. G. Measurement of Tensile Strength of Natural Rubber Vulcanizates at Elevated Temperature. *Rubber Chem. Technol.* **1982**, *55*, 66-75, doi:10.5254/1.3535876

[5] Thomas, A. G.; Whittle, J. M. Tensile Rupture of Rubber. *Rubber Chem. Technol.* **1970**, *43*, 222-228, doi:10.5254/1.3547249

[6] Hussein, M. Effects of strain rate and temperature on the mechanical behavior of carbon black reinforced elastomers based on butyl rubber and high molecular weight polyethylene. *Results Phys.* **2018**, *9*, 511-517, doi:10.1016/j.rinp.2018.02.043

[7] Ovalle Rodas, C.; Zaïri, F.; Naït-Abdelaziz, M.; Charrier, P. Temperature and filler effects on the relaxed response of filled rubbers: Experimental observations on a carbon-filled SBR and constitutive modeling. *Int. J. Solids Struct.* **2015**, *58*, 309-321, doi:10.1016/j.ijsolstr.2014.11.001

[8] Zhang, W.; Gong, X.; Xuan, S.; Jiang, W. Temperature-Dependent Mechanical Properties and Model of Magnetorheological Elastomers. *Ind. Eng. Chem. Res.* **2011**, *50*, 6704-6712, doi:10.1021/ie200386x

[9] Chu, H.; Hong, Y.; Chen, Q.; Wang, R. Establishment of rubber thermo-viscoelastic constitutive model and analysis of temperature field. *IOP Conf. Ser. Mater. Sci. Eng.* **2019**, *531*, 012042, doi:10.1088/1757-899x/531/1/012042

[10] Stevenson, A. The influence of low-temperature crystallization on the tensile elastic modulus of natural rubber. *J. Polym. Sci. Polym. Phys. Ed.* **1983**, *21*, 553-572, doi:10.1002/pol.1983.180210406

[11] D20 Committee Test Method for Brittleness Temperature of Plastics and Elastomers by Impact; ASTM International

[12] Barlow, C.; Jayasuriya, S. K.; Tan, C. S. *The world rubber industry*; Routledge: London ; New York, 1994; ISBN 978-0-415-02369-6

[13] Huang, Y.; Li, Y.; Zhao, H.; Wen, H. Research on constitutive models of hydrogenated nitrile butadiene rubber for packer at different temperatures. *J. Mech. Sci. Technol.* **2020**, *34*, 155-164, doi:10.1007/s12206-019-1217-x

[14] *ASM metals reference book*; Bauccio, M., American Society for Metals, Eds.; 3rd ed.; ASM International: Materials Park, Ohio, 1993; ISBN 978-0-87170-478-8

[15] *Rubber nano blends: preparation, characterization and applications*; Markovic, G., Visakh P. M., V. P., Eds.; Springer: Cham, 2017; ISBN 978-3-319-48720-5

[16] Hickman, J. A. *Polymeric seals and sealing technology*; Rapra review reports; Rapra Technology Ltd: Shawbury, Shrewsbury, 1997; ISBN 978-1-85957-096-8

[17] Chandrasekaran, C. Raw Materials for Rubber Lining Compounds. In *Anticorrosive Rubber Lining*; Chandrasekaran, C., Ed.; William Andrew Publishing, 2017; pp. 77-86 ISBN 978-0-323-44371-5

[18] Kanny, K.; Mohan, T. P. Rubber nanocomposites with nanoclay as the filler. In *Progress in Rubber Nanocomposites*; Thomas, S., Maria, H. J., Eds.; Woodhead Publishing, 2017; pp. 153-177 ISBN 978-0-08-100409-8

[19] Raut, P.; Swanson, N.; Kulkarni, A.; Pugh, C.; Jana, S. C. Exploiting arene-perfluoroarene interactions for dispersion of carbon black in rubber compounds. Polymer 2018, 148, 247-258, doi:10.1016/j.polymer.2018.06.025

[20] Delattre, A.; Lejeunes, S.; Lacroix, F.; Méo, S. On the dynamical behavior of filled rubbers at different temperatures: Experimental characterization and constitutive modeling. *Int. J. Solids Struct.* **2016**, *90*, 178-193, doi:10.1016/j.ijsolstr.2016.03.010

[21] Lion, A. On the large deformation behaviour of reinforced rubber at different temperatures. *J. Mech. Phys. Solids* **1997**, *45*, 1805-1834, doi:10.1016/S0022-5096(97)00028-8

[22] Martinez, J. M.; Boukamel, A.; Méo, S.; Lejeunes, S. Statistical approach for a hyper-visco-plastic model for filled rubber: Experimental characterization and numerical modeling. *Eur. J. Mech. - ASolids* **2011**, *30*, 1028-1039, doi:10.1016/j.euromechsol.2011.06.013

[23] Mullins, L. Effect of Stretching on the Properties of Rubber. *Rubber Chem. Technol.* **1948**, *21*, 281-300, doi:10.5254/1.3546914

[24] Chanliau-Blanot, M. T.; Nardin, M.; Donnet, J. B.; Papirer, E.; Roche, G.; Laurenson, P.; Rossignol, G. Temperature dependence of the mechanical properties of EPDM rubber-polyethylene blends filled with aluminium hydrate particles. *J. Mater. Sci.* **1989**, *24*, 649-657, doi:10.1007/BF01107456

[25] RP, B. Physical Testing of Rubber. *Phys. Test. Rubber* **2006**, 1-387, doi:10.1007/0-387-29012-5

[26] Pascual-Francisco, J. B.; Farfan-Cabrera, L. I.; Susarrey-Huerta, O. Characterization of tension set behavior of a silicone rubber at different loads and temperatures via digital image correlation. *Polym. Test.* **2020**, *81*, 106226, doi:10.1016/j.polymertesting.2019.106226

[27] Zhang, R. Elastic Parameters Measurement of Rubber by Digital Image Correlation. *Appl. Mech. Mater.* **2014**, *444-445*, 1532-1535, doi:10.4028/www.scientific.net/AMM.444-445.1532

[28] Large elastic deformations of isotropic materials VII. Experiments on the deformation of rubber. *Philos. Trans. R. Soc. Lond. Ser. Math. Phys. Sci.* **1951**, *243*, 251-288, doi:10.1098/rsta.1951.0004

[29] Darijani, H.; Naghdabadi, R.; Kargarnovin, M. H. Hyperelastic materials modelling using a strain measure consistent with the strain energy postulates. *Proc. Inst. Mech. Eng. Part C J. Mech. Eng. Sci.* **2010**, *224*, 591-602, doi:10.1243/09544062JMES1590

[30] Mooney, M. A Theory of Large Elastic Deformation. *J. Appl. Phys.* **1940**, *11*, 582-592, doi:10.1063/1.1712836

[31] Rivlin, R. S.; Rideal, E. K. Large elastic deformations of isotropic materials IV. further developments of the general theory. *Philos. Trans. R. Soc. Lond. Ser. Math. Phys. Sci.* **1948**, *241*, 379-397, doi:10.1098/rsta.1948.0024

[32] Rivlin, R. S.; Saunders, D. W. Large Elastic Deformations of Isotropic Materials. VII. Experiments on the Deformation of Rubber. *Philos. Trans. R. Soc. Lond. Ser. Math. Phys. Sci.* **1951**, *243*, 251-288

[33] Yeoh, O. H. Characterization of Elastic Properties of Carbon-Black-Filled Rubber Vulcanizates. *Rubber Chem. Technol.* **1990**, *63*, 792-805, doi:10.5254/1.353828

[34] Arruda, E. M.; Boyce, M. C. A three-dimensional constitutive model for the large stretch behavior of rubber elastic materials. *J. Mech. Phys. Solids* **1993**, *41*, 389-412, doi:10.1016/0022-5096(93)90013-6

[35] Boyce, M. C.; Arruda, E. M. Constitutive Models of Rubber Elasticity: A Review. *Rubber Chem. Technol.* **2000**, *73*, 504-523, doi:10.5254/1.3547602

[36] Treloar, L. R. G. The elasticity of a network of long-chain molecules—II. *Trans Faraday Soc* **1943**, *39*, 241-246, doi:10.1039/TF9433900241

[37] Li, X.; Dong, Y.; Li, Z.; Xia, Y. Experimental study on the temperature dependence of hyperelastic behavior of tire rubbers under moderate finite deformation. *Rubber Chem. Technol.* **2011**, *84*, 215-228, doi:10.5254/1.3577534

[38] Mansouri, M. R.; Darijani, H. Constitutive modeling of isotropic hyperelastic materials in an exponential framework using a self-contained approach. *Int. J. Solids Struct.* **2014**, *51*, 4316-4326, doi:10.1016/j.ijsolstr.2014.08.018

[39] Kelley, C. T. *Iterative methods for optimization*; Frontiers in applied mathematics; SIAM: Philadelphia, 1999; ISBN 978-0-89871-433-3

[40] Levenberg, K. A method for the solution of certain non-linear problems in least squares. *Q. Appl. Math.* **1944**, *2*, 164-168, doi:10.1090/qam/10666

[41] Marquardt, D. W. An Algorithm for Least-Squares Estimation of Nonlinear Parameters. *J. Soc. Ind. Appl. Math.* **1963**, *11*, 431-441, doi:10.1137/0111030

[42] Kanzow, C.; Yamashita, N.; Fukushima, M. Levenberg–Marquardt methods with strong local convergence properties for solving nonlinear equations with convex constraints. *J. Comput. Appl. Math.* **2004**, *172*, 375-397, doi:10.1016/j.cam.2004.02.013